Hindawi
Journal of Nanomaterials
Volume 2022, Article ID 6405772, 8 pages
https://doi.org/10.1155/2022/6405772

Research Article

An *In Vitro* Study on the Antibacterial Effects of Chlorhexidine-Loaded Positively Charged Silver Nanoparticles on *Enterococcus faecalis*

Ahmad Gholami,[1,2,3] **Keyvan Ghezelbash**,[4] **Bahar Asheghi**,[4] **Abbas Abbaszadegan**,[4] **and Abbas Amini**[5]

[1]*Biotechnology Research Center, Shiraz University of Medical Sciences, Shiraz, Iran*
[2]*Pharmaceutical Sciences Research Center, Shiraz University of Medical Sciences, Shiraz, Iran*
[3]*Department of Pharmaceutical Biotechnology, School of Pharmacy, Shiraz University of Medical Sciences, Shiraz, Iran*
[4]*Department of Endodontics, Shiraz Dental School, Shiraz University of Medical Sciences, Shiraz, Iran*
[5]*Centre for Infrastructure of Engineering, Western Sydney University, Penrith, NSW 2751, Australia*

Correspondence should be addressed to Bahar Asheghi; asheghib@sums.ac.ir
and Abbas Abbaszadegan; dr.abbaszadegan@gmail.com

Received 6 January 2022; Revised 25 April 2022; Accepted 26 June 2022; Published 25 July 2022

Academic Editor: Isaac Acquah

This study successfully developed a positively charged silver nanocomplex as a nanocarrier for chlorhexidine (CHX) using ionic liquids. This nanocomplex can interestingly deliver the antibacterial agent with a synergistic effect. In this study, we synthetized and characterized a positively charged silver nanocomplex ($AgNPs^+$) and CHX-loaded positively charged silver nanoparticles ($CHX@AgNPs^+$) using UV-visible spectroscopy, transmission electron microscopy, X-ray diffractometer, Fourier transform infrared spectroscopy, and Zetasizer. Then, the loading efficiency and release profile of XHX from nanocomplex were evaluated. The antibacterial activity was evaluated by employing two standard microdilution tests to obtain the minimum bactericidal and inhibitory concentrations. The average sizes of 27.43 nm and 29.66 nm were obtained for $AgNPs^+$ and $CHX@AgNPs^+$, respectively. The $CHX@AgNPs^+$ showed a constant release of CHX, making them a more effective antibacterial agent against *Enterococcus faecalis* (*E. faecalis*) than CHX or $AgNPs^+$ alone. Antibacterial assays showed that $CHX@AgNPs^+$ significantly reduced the viability of the bacterial strain compared to CHX as the standard irrigant. $AgNPs^+$ had an antibacterial effect similar to CHX only at intermediate concentrations (12 and 25 μg/mL), and their effects were significantly less than those of CHX at other concentrations (3, 6, 50, and 100 μg/mL). The effects of $CHX@AgNPs^+$ were statistically greater than those of $AgNPs^+$ at all concentrations tested. The MIC values of $CHX@AgNPs^+$ and CHX were 50 and 100 μg/mL. However, $AgNPs^+$ were not showed MIC value at tested concentrations. Therefore, the designed nanocomplex can be regarded as a potential root canal disinfectant with clinical applications for bacterial infections.

1. Introduction

Bacterial elimination in infected root canal systems is performed using mechanical debridement and chemical elimination of intraradicular microorganisms [1]. As a very resistant microorganism in infected root canals, *Enterococcus faecalis* (*E. faecalis*) can stubbornly survive lethal challenges and invade dentinal tubules, making it the most persistent pathogen in root canal treatment [2].

For the chemomechanical preparation of the root canal system, one or more antibacterial irrigants may be used to enhance intracanal disinfection. Ethylenediaminetetraacetic

acid (EDTA), chlorhexidine (CHX), and sodium hypochlorite (NaOCl) are the most frequently used root canal irrigation solutions for removing bacteria from infected canals. NaOCl and EDTA remove the smear layer from the infected canals. NaOCl also has a tissue dissolution capability [3, 4]. The principal downside of NaOCl is its nasty odor and taste along with its caustic effect particularly when it is extruded from the apical region. Although CHX is an interesting irrigant with an effective antibacterial activity, previous studies have demonstrated that it has a toxic effect on some eukaryotic cells [5]. Besides, its activity is pH sensitive and it should be prescribed with care due to the risk of bacterial resistance [6]. Although many studies have been conducted on intracanal preparation and canal irrigants, no ideal endodontic irrigant has been found yet [7].

Silver nanoparticles (AgNPs) have a strong and broad-spectrum antibacterial activity. As a result, they have been employed in several fields including dentistry [8]. It has been speculated that AgNPs interfere with oxygen uptake and bacterial cell wall integrity due to their ability to bind with enzymes and proteins [9]. Furthermore, many studies have demonstrated that Ag particles at the nanoscale are compatible with human cells in minute concentrations [10]. In addition, the surface charge of AgNPs and their magnitude play a significant role in the level of their antibacterial activity [11].

One of the most significant global threats is antibacterial resistance [12]. To counter antibacterial resistance, it is required that new drug development strategies such as combination therapies be implemented. One technique to improve the efficacy of antibacterial agents is to combine them in order to counter the rising rates of resistance to conventional antibacterial agents [13]. Combination therapies are different in terms of the number of their components and the targeted pathways [14].

Previous studies have shown the synergistic effects of antibacterial agents in dental treatments. Lu et al. demonstrated the synergistic effects of CHX and AgNPs against peri-implantitis pathogens [15]. Moreover, another study showed that the mixture of calcium and nanosilver can have good and residual antibacterial properties after one week compared with the other groups [16]. Combining CHX and silver ions can increase their effectiveness and improve the quality of endodontic treatment [17].

A suitable nanocarrier for antibacterial compounds that can target infection foci in the root canal microenvironment is one of the necessities of modern endodontic treatment [18].

This *in vitro* study was designed to (i) synthesize and characterize AgNPs with a positive charge and a CHX molecule loaded on them (CHX@$AgNPs^+$) and (ii) to evaluate their antibacterial efficacy by determining their minimum bactericidal concentration (MBC) and minimum inhibitory concentration (MIC) against *E. faecalis* and comparing them with those of CHX and $AgNPs^+$ alone.

2. Materials and Methods

2.1. Synthesis and Characterization. In order to synthesize the positively charged NPs, 1.0 mL of an aqueous solution of $AgNO_3$ (Sigma-Aldrich Co., St. Louis, MO, USA, 0.01 M) was mixed and stirred with 6.2 mM 1-dodecyl-3-methylimidazolium chloride (Sigma-Aldrich Co., USA) according to our previous study [19]. The prepared 0.4 M $NaBH_4$ aqueous solution was next instantly added dropwise to the stirred solutions till a golden color was resulted. Afterward, to remove the remaining ionic liquids, the colloidal solutions were centrifuged for approximately 20 min.

An alcoholic solution of CHX (Sigma-Aldrich Co., USA, 1.5 mg/mL) was prepared and poured on the alcoholic suspension of $AgNPs^+$ (2 mg/mL) and stirred for 24 h at room temperature using a magnetic stirrer. Finally, the obtained suspension was dried at 40°C in the oven and kept in a dark container in the refrigerator for antibacterial studies. Before the antibacterial studies, the powder was suspended in sterile distilled water.

Several analytical instruments were used in order to characterize the synthesized nanoparticles. UV-visible spectroscopy is a simple and common technique to verify the formation of nanoparticles. In the current research, distilled water was used as a reference. A UV-1800 UV-visible spectrometer (Shimadzu Corporation, Kyoto, Japan) was employed to obtain the absorbance spectrum of the colloidal sample which was found to range from 200 to 800 nm.

The transmission electron microscopy (TEM) analysis was performed in order to determine the morphology, shape, and size of AgNPs. The TEM measurements were performed using a HITACHI H-800 microscope which operated at 200 kV. In order to prepare the TEM grid, a drop of the diluted solution was placed on a carbon-coated copper grid and then dried under a lamp.

A Siemens D5000 diffractometer (Karlsruhe, Germany) was employed for the X-ray diffraction (XRD) analysis using monochromatic Cu kα radiation ($\lambda = 1.5406$ Å) which operated at 40 kV and 30 mA at a 2θ angle pattern. The scanning range was from 20° to 80°. A comparison was performed between the obtained images and the database of Joint Committee on Powder Diffraction Standards (JCPDS) so that the crystalline structure could be explained.

The Fourier transform infrared spectroscopy (FT-IR spectroscopy) analysis was conducted to classify the compounds responsible both for the stabilization of nanoparticles and the reduction of metals. A Vertex 70 (Bruker, Germany) in the wavelength range of 400-4000 cm^{-1} was employed to analyze the functional group at the surface of AgNPs.

Using a Zetasizer (Nano ZS-90, Malvern Instruments, UK), the zeta potentials of the nanoparticles were determined. 700 μL AgNP suspensions were freshly prepared and analyzed at 25°C with a scattering angle of 90°.

2.2. CHX Loading Efficiency. UV/VIS was used to evaluate the loading efficiency of CHX on $AgNPs^+$ at the wavelength of 254 nm. Accordingly, the amount of unloaded CHX after the loading procedure was calculated and the CHX loading percentage was presented using the following equation from the study of Gholami et al. [20]:

$$\text{Loading efficiency}\ (\%) = \frac{(\text{total concentration of CHX} - \text{concentration of unloaded CHX})}{\text{concentration of CHX}}. \quad (1)$$

2.3. CHX Release Profile. Based on the study of Gholami et al. [20], UV/VIS at 254 nm was used to assess the release behavior of CHX on $AgNPs^+$. 20 mg of CHX@$AgNPs^+$ in a dialysis bag (with a cutoff of 100 kDa) was placed in PBS (50 mL) for 7 days at 37°C, and the rate of drug release was measured at predetermined time points. At these time points, 1 mL PBS was taken from the container and the released CHX was reported.

2.4. Antibacterial Study through the Determination of MIC and MBC. The MBC and MIC of each experimental solution against planktonic *E. faecalis* were obtained three times by a microdilution broth method. The tested solutions were 0.2% CHX, $AgNPs^+$, and synthesized CHX@$AgNPs^+$. All the tests were conducted according to the instructions of the Clinical and Laboratory Standards Institute (CLSI). In order to obtain the MIC, 2-fold serial dilutions (up to seven times) of the experimental solutions and the control group were prepared using Mueller-Hinton broth (MHB) in 96-well microplates. To obtain a volume of 90 μL, *E. faecalis* was cultured in BHI broth and the turbidity was set to 0.11-0.13 at an optical density (OD) of 600, resulting in 1.5×10^8 colony forming units per milliliter (CFU/mL) of bacteria. Then, the suspension was diluted 1 : 20 with broth culture. Eventually, 10 μL of *E. faecalis* suspension was added to each microplate and incubated at 37°C. After 24 hours, a microplate reader was used to record the absorbance at a wavelength of 600 nm to evaluate the inhibitory effects of the test solutions. The positive control group consisted of *E. faecalis* inoculated culture media, while the negative control group was composed of culture media without microorganisms. The least concentration of each experimental solution inhibiting 90% of *E. faecalis* growth compared with the negative control group was defined as the MIC value.

To quantify the level of MBC for the test irrigants, the experimental solutions with equal and higher concentrations than the MICs were placed on tryptic soy agar plates and incubated at 37°C. The colonies were counted after 24 hours. The MBC value was defined as the least concentration leading to the almost complete elimination of the microorganisms in the primary inocula. This happened when less than 4 visible colonies were detectable in the agar plates after 24 h of incubation at 37°C.

2.5. Statistical Analysis. The one-way ANOVA was used to compare the antibacterial agents. Tukey's post hoc test was utilized to analyze the data. In addition, the SPSS statistical software (IBM, version: 19.0) was employed to evaluate the results. The P value of <0.05 was assumed a significant difference, and the test was repeated thrice.

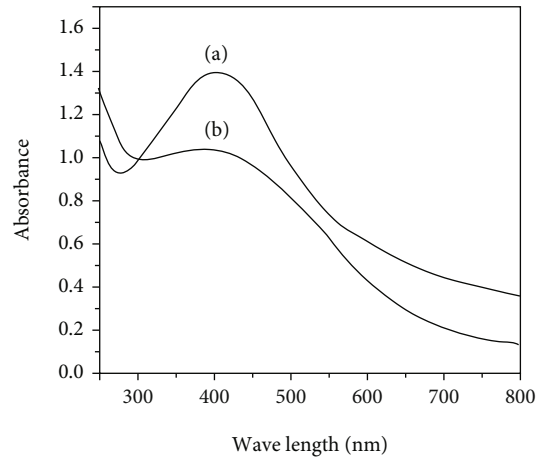

Figure 1: UV-visible spectroscopy of (a) $AgNPs^+$ and (b) CHX@$AgNPs^+$.

3. Results

3.1. Synthesis and Characterization of the Nanostructures. Positively charged silver nanoparticles with a relatively uniform spherical morphology were synthesized according to Gholami et al. [19]. The UV-visible spectroscopy of $AgNPs^+$ and CHX@$AgNPs^+$ is shown in Figure 1. A UV-vis spectrophotometer was employed to observe and record the synthesis process of AgNPs from 300 to 800 nm. During the reduction process, a characteristic absorption peak at around 400-450 nm resulted from the surface plasmon resonance (SPR) marked the formation of AgNPs [21]. The intensity of this peak was strongly correlated with the three factors of particle size, solvent dielectric constant, and chemical structure. AgNPs possess free electrons that result in a SPR absorption band that can be observed by a UV-vis spectrophotometer because of the mutual vibration of electrons in resonance with the light wave [22]. In this study, in the graphs of both $AgNPs^+$ and CHX@$AgNPs^+$, this characteristic peak appears in regions with a wavelength of about 450 nm. This wavelength range is in accordance with several previous studies [10, 19, 23].

As shown in Figure 2, the TEM micrographs of $AgNPs^+$ and CHX@$AgNPs^+$ represent spherical particles. To obtain the average sizes of the nanoparticles, 30 isolated nanoparticles in each figure were measured. The average sizes of 27.43 nm and 29.66 nm were obtained for $AgNPs^+$ and CHX@$AgNPs^+$, respectively. The TEM images revealed that the average sizes of $AgNPs^+$ and CHX@$AgNPs^+$ were approximately equal.

CHX was loaded on the surface of $AgNPs^+$ probably by introducing the cationic groups of ionic liquid into the CHX solution. The surface functionalization of positively charged CHX on $AgNPs^+$ may be due to the weak van der Waals forces such as lipophilic (between the alkyl chain of the CHX structures and the poly alkyl chain of the ionic liquid on $AgNPs^+$) and/or electrostatic interactions (between the Cl^- groups in the CHX molecule and the NH_3^+ groups in the imidazolium structure). Further studies are needed

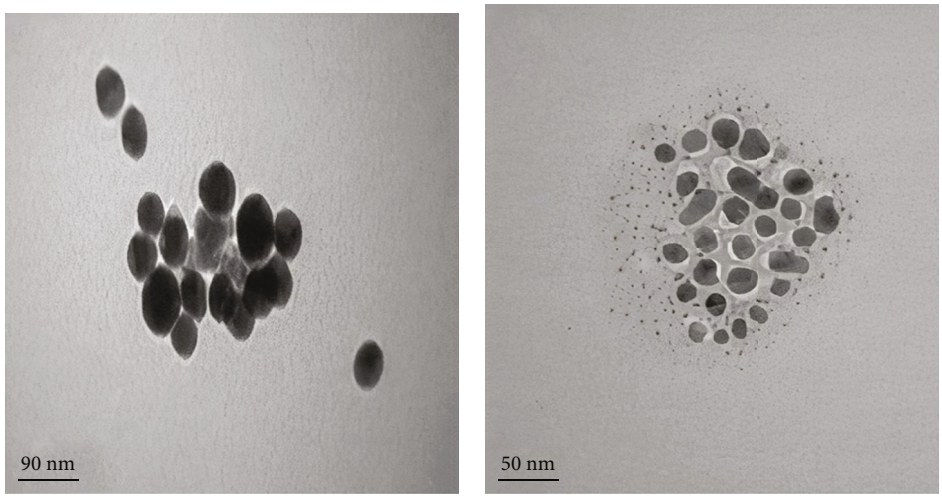

(a) (b)

Figure 2: The TEM images of (a) $AgNPs^+$ and (b) $CHX@AgNPs^+$.

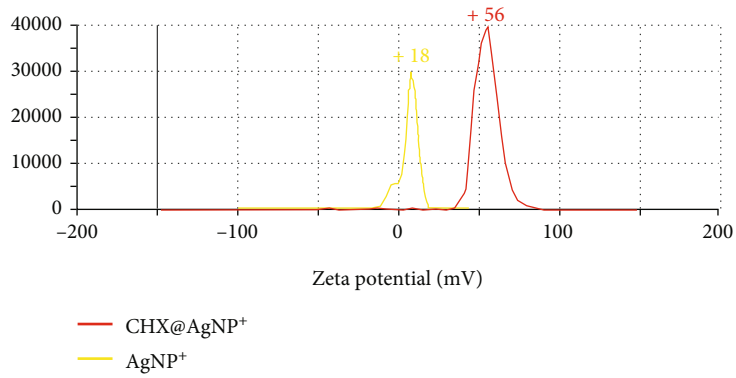

Figure 3: The zeta potentials of the $AgNPs^+$ and $CHX@AgNPs^+$.

to prove and accurately determine these interactions. However, the increase of the zeta potential after the functionalization of $AgNPs^+$ with CHX may partially confirm this claim.

In fact, using a DLS device, the zeta potentials of $AgNPs^+$ and $CHX@AgNPs^+$ were obtained as +18 mV and +56 mV, respectively. By adding CHX to $AgNPs^+$, the zeta potential increased from +18 mV to +56 mV due to the interaction between the cations of $AgNPs^+$ and CHX (with two cationic centers) containing 10 N atoms. The amplification of the zeta potential could also show that CHX intercalated within the alkylated AgNPs and altered their surfaces (Figure 3).

The wide-angle XRD pattern of the resulted AgNPs at a 2θ range of 20°-80° at room temperature revealed the intensity diffraction peaks at 38°, 44°, 65°, and 78° which corresponded to (111), (200), (220, 311) planes, respectively (Figure 4).

The functional groups involved in the stabilization, capping, surface, and reduction of AgNPs were confirmed by FT-IR analysis (Figure 5). As shown in graph 4a, there are characteristic peaks for $AgNPs^+$ at 3402, 2920, and 1644 cm^{-1}. The peak at 3402 cm^{-1} in the $AgNPs^+$ is associated with the N-H bond of amide and the O-H bond of

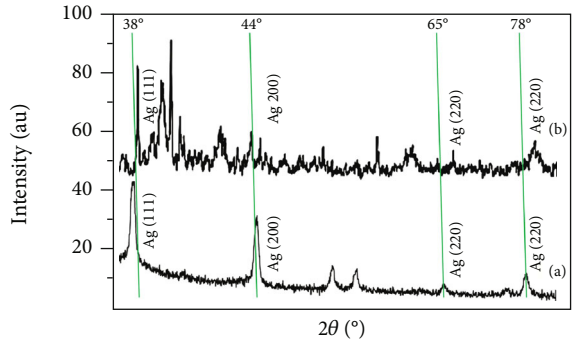

Figure 4: The XRD patterns of (a) $AgNPs^+$ and (b) $CHX@AgNPs^+$.

the hydroxy groups which extend to the surface imidazolium groups. Furthermore, the vibrations at around 2920 cm^{-1} can be associated with the stretching aliphatic CH bands which exist in the cationic aliphatic side chain. The peak that appears at about 1644 cm^{-1} also confirms the presence of an acrylic carbonyl group of $AgNPs^+$. This peak also appears in the graph of $CHX@AgNPs^+$.

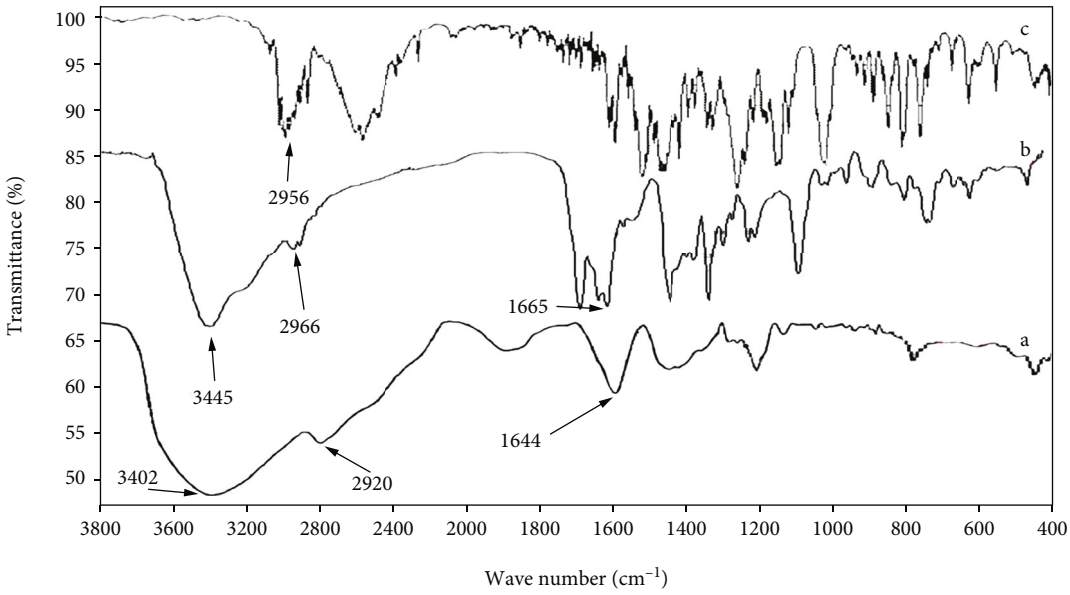

Figure 5: The FT-IR spectra of (a) AgNPs$^+$, (b) CHX@AgNPs$^+$, and (c) CHX with a KBr tablet in the region of 400-4000 cm^{-1}.

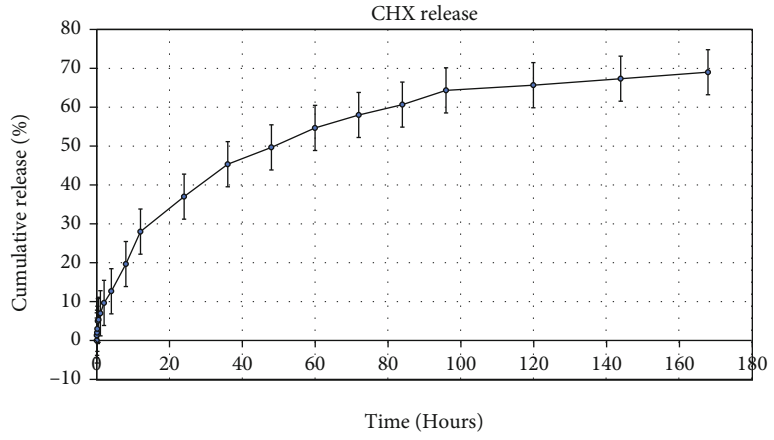

Figure 6: The release profile of CHX from CHX@AgNPs$^+$ during 180 hours.

3.2. The Loading Efficiency and Release Profile of CHX. Ideal drug carriers efficiently attach to the microbial cell membrane and adequately release the antibacterial agent. To achieve sufficient release of CHX, the aliphatic ionic liquid was introduced to the surface of AgNPs$^+$ to load CHX through electrostatic interaction. The UV-vis measurement revealed that the loading efficiency of CHX on AgNPs$^+$ was 86.7 ± 13.2.

The release profile of CHX from CHX@AgNPs$^+$ is interesting. As shown in Figure 6, an initial rapid release pattern occurred for CHX during the first 8 hours. About 20% of CHX was cumulatively released after 8 hours, whereas 37% of CHX was released after 24 hours. This fast release may be due to the dissociation and protonation of the carboxyl functional groups, resulting in the preferential release of CHX.

3.3. The Assessment of Antibacterial Activity. Based on the results of the broth microdilution test, the three experimental solutions all inhibited the growth of *E. faecalis* significantly in comparison with the control group. The MIC values of all the tested solutions were similar to their MBC values. The smallest MIC and MBC values belonged to CHX@AgNPs$^+$ (50 μg/mL), followed by CHX (100 μg/mL) and AgNPs$^+$ (N/A). In their initial concentration, AgNPs$^+$ could not inhibit 90% of *E. faecalis*. Thus, the exact MBC and MIC values for AgNPs$^+$ could not be determined. The statistical analysis showed that in most concentrations (except for 100 μg/mL), CHX@AgNPs$^+$ significantly reduced the viability of the bacterial strain compared to CHX as the standard irrigant. On the other hand, AgNPs$^+$ had an antibacterial effect similar to CHX only at intermediate concentrations (12 and 25 μg/mL) and their

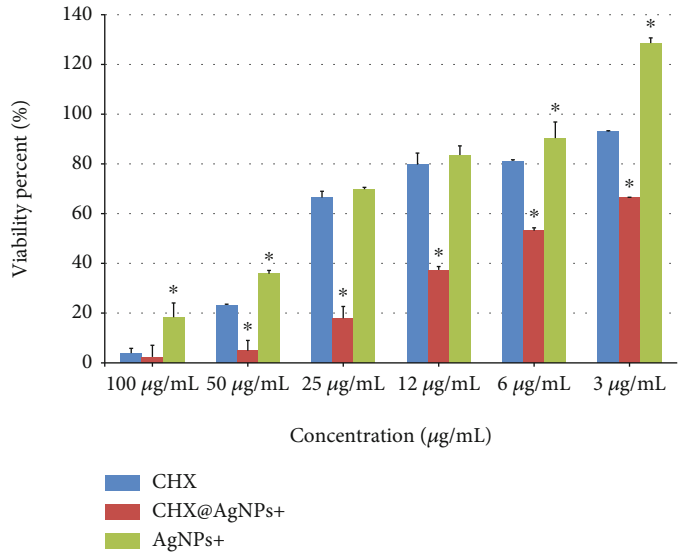

Figure 7: The viability of *E. faecalis* when treated with different concentrations of experimental solutions. *Statistically significant difference between the CHX (as the standard antibacterial irrigant) and other groups.

effects were significantly less than those of CHX at other concentrations (3, 6, 50, and 100 μg/mL). The effects of CHX@AgNPs$^+$ were statistically greater than those of AgNPs$^+$ at all concentrations tested. Figure 7 summarizes the details.

4. Discussion

In endodontics, the use of intracanal disinfectant solutions with adequate efficacy and acceptable biocompatibility will lead to the eradication of resistant microorganisms within the root canal and periapical areas and will consequently decrease the failure rate of root canal treatment [17].

The use of AgNPs has increased in many fields including dentistry. It is speculated that the antibacterial nanoscale structures do not allow the bacteria to resist [24]. Therefore, many studies have mentioned AgNPs as an effective and appropriate medication for endodontic purposes [25]. In the present preliminary *in vitro* study, the possible synergistic impacts of AgNPs$^+$ and CHX were investigated since both of these substances have a strong antibacterial activity. Lu et al. showed that CHX-loaded silver-decorated mesoporous silica nanoparticles (Ag-MSNs@CHX) had a pH-responsive release of silver ions and CHX simultaneously. This resulted in synergistically antibacterial effects against both Gram-negative *Escherichia coli* and Gram-positive *Staphylococcus aureus* [15]. Another study demonstrated the effective antibacterial activity of a novel CHX-AgNP solution which could be an effective antibacterial agent against endodontic flora [26].

This study used positively charged AgNPs and synthesized a new structure with a spherical shape and size of 20-30 nm. Recent studies have confirmed that the physicochemical characteristics of AgNPs$^+$ (including crystal structure, shape, surface morphology, zeta potential, size, and surface charge) are significant factors that affect their antibacterial activity [23, 27–29]. Besides, it was demonstrated that positively charged AgNPs could have a greater antibacterial efficacy against *E. faecalis* and have an outstanding level of biocompatibility [25].

In this study, CHX was also loaded on AgNPs$^+$ due to its strong antibacterial and synergistic effect. CHX@AgNPs$^+$ was synthesized and characterized, and then, the antibacterial effect of this solution on *E. faecalis* was assessed in order to determine its MIC and MBC values compared to those of CHX and AgNPs$^+$ alone. *E. faecalis* was selected based on previous studies that associated this microorganism with recurrent infections after root canal treatments [30].

Our results revealed that the MBC and MIC values of CHX@AgNPs$^+$ were less than those of CHX and AgNPs$^+$ alone. The MBC and MIC values of CHX@AgNP$^+$s were similar (50 μg/mL), while CHX was less effective with the MBC and MIC values of 100 μg/mL. For the AgNPs$^+$, we were not able to determine the exact MIC and MBC values during the serial dilutions. This means that this agent, even at its initial concentration, was not enough in inhibiting the growth of 90% of the bacteria.

The greater effectiveness of the CHX@AgNPs$^+$ solution on the microorganism compared to the other tested irrigants might be attributed to the electrostatic repulsion between CHX and AgNPs$^+$ due to their total electrical surface charge that may result in a lower aggregation of particles, more surface area, and minimization of the interaction time, destroying the microorganism with optimal effectiveness [31]. Additionally, the negatively charged components in the structure of Gram-positive bacterial cell walls and cell membrane (including teichoic acid, lipoteichoic acid, carboxyl, and phosphate groups) [9, 32] act as a target for the positive charge of the synthesized particle, leading to the disturbance of cell wall permeability, formation of proteinaceous pores, and destruction of the bacterial organism due to the leakage of intracellular contents. These findings

were in agreement with those of former studies focusing on the effect of surface charge on the bactericidal efficacy of NPs [9, 19, 27].

Suitable nanocarriers bind to bacterial surfaces and quickly release antibiotics or antiseptics in reaction to any stimulus. Based on the release profile of CHX, a new antibacterial solution was made to irrigate the root canal during the treatment process. The solution was expected to have rapid antibacterial properties. Since time is limited in clinical work, a fast release can be beneficial and more CHX can come in contact with the root canal system.

To sum up, the current study demonstrated that CHX@AgNPs^{+} had an excellent antibacterial effect on *E. faecalis*. In the current in vitro study, we tried to integrate nanoscience, chemistry, and bacteriology to obtain a new disinfectant for endodontic purposes. However, since the root canal ecosystem is a complex environment, further studies on the effect of CHX@AgNPs^{+} on infected *ex vivo* models and other bacterial species as well as cytocompatibility assessments of CHX@AgNPs^{+} against human cells are needed to evaluate its application as a new disinfectant in endodontics adequately.

5. Conclusion

Within the limitations of the present research, we can state that CHX@AgNPs^{+}, whose MBC and MIC values are significantly lower than those of CHX and AgNPs^{+} alone, can be regarded as a potential root canal disinfectant. Further studies are needed to confirm the results of the present study regarding this agent when it is used in *ex vivo* models and against bacterial biofilm.

Data Availability

All data used to support the findings of this study are included within the article.

Conflicts of Interest

The authors declare that they have no conflicts of interest.

Acknowledgments

The authors of this paper would like to appreciate the Vice-Chancellery of Shiraz University of Medical Sciences for supporting this study (Ethics Committee Approval: #IR.SUMS.DENTAL.REC.1399.071; Grant: #20450).

References

[1] F. Mohammadi, A. Abbaszadegan, and A. Gholami, "Recent advances in nanodentistry: a special focus on endodontics," *Micro & Nano Letters*, vol. 15, no. 12, pp. 812–816, 2020.

[2] A. Abbaszadegan, S. Sahebi, A. Gholami et al., "Time-dependent antibacterial effects of Aloe vera and Zataria multiflora plant essential oils compared to calcium hydroxide in teeth infected with Enterococcus faecalis," *Journal of Investigative and Clinical Dentistry*, vol. 7, no. 1, pp. 93–101, 2016.

[3] M. Nabavizadeh, A. Abbaszadegan, A. Gholami et al., "Chemical constituent and antimicrobial effect of essential oil from Myrtus communis leaves on microorganisms involved in persistent endodontic infection compared to two common endodontic irrigants: an in vitro study," *Journal of conservative dentistry: JCD*, vol. 17, no. 5, pp. 449–453, 2014.

[4] M. Sedigh-Shams, A. Gholami, A. Abbaszadegan et al., "Antimicrobial efficacy and cytocompatibility of calcium hypochlorite solution as a root canal irrigant: an in vitro investigation," *Iranian endodontic journal*, vol. 11, no. 3, pp. 169–174, 2016.

[5] A. Abbaszadegan, A. Gholami, Y. Ghahramani et al., "Antimicrobial and cytotoxic activity of Cuminum cyminum as an intracanal medicament compared to chlorhexidine gel," *Iranian endodontic journal*, vol. 11, no. 1, pp. 44–50, 2016.

[6] F. Cieplik, N. S. Jakubovics, W. Buchalla, T. Maisch, E. Hellwig, and A. al-Ahmad, "Resistance toward chlorhexidine in oral bacteria–is there cause for concern?," *Frontiers in Microbiology*, vol. 10, p. 587, 2019.

[7] A. Abbaszadegan, Y. Ghahramani, M. Farshad, M. Sedigh-Shams, A. Ghomali, and A. Jamshidzadeh, "In vitro evaluation of dynamic viscosity, surface tension and dentin wettability of silver nanoparticles as an irrigation solution," *Iranian Endodontic Journal*, vol. 14, no. 1, pp. 23–27, 2019.

[8] N. Ebrahimi, S. Rasoul-Amini, A. Ebrahiminezhad, Y. Ghasemi, A. Gholami, and H. Seradj, "Comparative study on characteristics and cytotoxicity of bifunctional magnetic-silver nanostructures: synthesized using three different reducing agents," *Acta Metallurgica Sinica (English Letters)*, vol. 29, no. 4, pp. 326–334, 2016.

[9] A. Abbaszadegan, A. Gholami, S. Abbaszadegan et al., "The effects of different ionic liquid coatings and the length of alkyl chain on antimicrobial and cytotoxic properties of silver nanoparticles," *Iranian endodontic journal*, vol. 12, no. 4, pp. 481–487, 2017.

[10] S. N. Abootalebi, S. M. Mousavi, S. A. Hashemi, E. Shorafa, N. Omidifar, and A. Gholami, "Antibacterial effects of green-synthesized silver nanoparticles using ferula asafoetida against Acinetobacter baumannii isolated from the hospital environment and assessment of their cytotoxicity on the human cell lines," *Journal of Nanomaterials*, vol. 2021, 12 pages, 2021.

[11] A. Abbaszadegan, Y. Ghahramani, A. Gholami et al., "The effect of charge at the surface of silver nanoparticles on antimicrobial activity against gram-positive and gram-negative bacteria: a preliminary study," *Journal of Nanomaterials*, vol. 2015, article 720654, 2015.

[12] P. Fan, Z. Ma, A. J. Partow et al., "A novel combination therapy for multidrug resistant pathogens using chitosan nanoparticles loaded with β-lactam antibiotics and β-lactamase inhibitors," *International Journal of Biological Macromolecules*, vol. 195, pp. 506–514, 2022.

[13] A. Gholami, A. Ebrahiminezhad, N. Abootalebi, and Y. Ghasemi, "Synergistic evaluation of functionalized magnetic nanoparticles and antibiotics against Staphylococcus aureus and Escherichia coli," *Pharmaceutical nanotechnology*, vol. 6, no. 4, pp. 276–286, 2018.

[14] M. A. Fischbach, "Combination therapies for combating antimicrobial resistance," *Current Opinion in Microbiology*, vol. 14, no. 5, pp. 519–523, 2011.

[15] M. Lu, Y. Ge, and C. Tang, "Synergistically antibacterial effect of chlorhexidine-loaded, silver-decorated mesoporous silica nanoparticles against peri-implantitis pathogens," *Clinical Oral Implants Research*, vol. 29, no. S17, pp. 53–53, 2018.

[16] F. Afkhami, G. Rostami, S. Batebi, and A. Bahador, "Residual antibacterial effects of a mixture of silver nanoparticles/calcium hydroxide and other root canal medicaments against Enterococcus faecalis," *Journal of Dental Sciences*, vol. 17, no. 3, pp. 1260–1265, 2021.

[17] K. Yousefi, H. D. Manesh, A. R. Khalifeh, and A. Gholami, "Fabrication and characterization of a nanofast cement for dental restorations," *International*, vol. 2021, pp. 1–12, 2021.

[18] W. Zakrzewski, M. Dobrzyński, A. Zawadzka-Knefel et al., "Nanomaterials Application in Endodontics," *Materials (Basel)*, vol. 14, no. 18, p. 5296, 2021.

[19] A. Gholami, M. S. Shams, A. Abbaszadegan, and M. Nabavizadeh, "Ionic liquids as capping agents of silver nanoparticles. Part II: antimicrobial and cytotoxic study," *Green Processing and Synthesis*, vol. 10, no. 1, pp. 585–593, 2021.

[20] A. Gholami, F. Emadi, M. Nazem et al., "Expression of key apoptotic genes in hepatocellular carcinoma cell line treated with etoposide-loaded graphene oxide," *Journal of Drug Delivery Science and Technology*, vol. 57, article 101725, 2020.

[21] K. Anandalakshmi, J. Venugobal, and V. Ramasamy, "Characterization of silver nanoparticles by green synthesis method using Pedalium murex leaf extract and their antibacterial activity," *Applied Nanoscience*, vol. 6, no. 3, pp. 399–408, 2016.

[22] R. Das, S. S. Nath, D. Chakdar, G. Gope, and R. Bhattacharjee, "Synthesis of silver nanoparticles and their optical properties," *Journal of Experimental Nanoscience*, vol. 5, no. 4, pp. 357–362, 2010.

[23] M. Nabavizadeh, A. Abbaszadegan, A. Gholami et al., "Antibiofilm efficacy of positively charged imidazolium-based silver nanoparticles in enterococcus faecalis using quantitative real-time PCR," *Journal of Microbiology*, vol. 10, no. 10, 2017.

[24] M. K. Rai, S. D. Deshmukh, A. P. Ingle, and A. K. Gade, "Silver nanoparticles: the powerful nanoweapon against multidrug-resistant bacteria," *Journal of Applied Microbiology*, vol. 112, no. 5, pp. 841–852, 2012.

[25] A. Adl, A. Abbaszadegan, A. Gholami, F. Parvizi, and Y. Ghahramani, "Effect of a new imidazolium-based silver nanoparticle irrigant on the bond strength of epoxy resin sealer to root canal dentine," *Iranian Endodontic Journal*, vol. 14, no. 2, pp. 122–125, 2019.

[26] S. Charannya, D. Duraivel, K. Padminee, S. Poorni, C. Nishanthine, and M. R. Srinivasan, "Comparative evaluation of antimicrobial efficacy of silver nanoparticles and 2% chlorhexidine gluconate when used alone and in combination assessed using agar diffusion method: an in vitro study," *Contemporary clinical dentistry*, vol. 9, Suppl 2, pp. S204–S209, 2018.

[27] A. Abbaszadegan, M. Nabavizadeh, A. Gholami et al., "Positively charged imidazolium-based ionic liquid-protected silver nanoparticles: a promising disinfectant in root canal treatment," *International Endodontic Journal*, vol. 48, no. 8, pp. 790–800, 2015.

[28] M. Guzman, J. Dille, and S. Godet, "Synthesis and antibacterial activity of silver nanoparticles against gram- positive and gram-negative bacteria," *Nanomedicine: Nanotechnology, Biology and Medicine*, vol. 8, no. 1, pp. 37–45, 2012.

[29] C. V. Restrepo and C. C. Villa, "Synthesis of silver nanoparticles, influence of capping agents, and dependence on size and shape: a review," *Environmental Nanotechnology, Monitoring & Management*, vol. 15, article 100428, 2021.

[30] Y. Ghahramani, N. Mohammadi, A. Gholami, and D. Ghaffaripour, "Antimicrobial efficacy of intracanal medicaments against E. faecalis bacteria in infected primary molars by using real-time PCR: a randomized clinical trial," *International Journal of Dentistry*, vol. 2020, 6 pages, 2020.

[31] S. Zargarnezhad, A. Gholami, M. Khoshneviszadeh, S. N. Abootalebi, and Y. Ghasemi, "Antimicrobial activity of isoniazid in conjugation with surface-modified magnetic nanoparticles against Mycobacterium tuberculosis and nonmycobacterial microorganisms," *Journal of Nanomaterials*, vol. 2020, 9 pages, 2020.

[32] B. Bechinger and S.-U. Gorr, "Antimicrobial peptides: mechanisms of action and resistance," *Journal of Dental Research*, vol. 96, no. 3, pp. 254–260, 2017.